Frontiers in Health Informatics
ISSN-Online: 2676-7104
www.healthinformaticsjournal.com
2024; Vol 13: Issue 7
Open Access

Preparation and optimization of telmisartan loaded solid lipid nanoparticles by central composite design

Noel Vinay Thomas[1], A Salomy Monica Diyya[2], Shahin Vahora[3], J.K. Shyamala[4], Shreya Arora[5], Harpreet Kaur[5], Ram C Dhakar[6] and V. Kalvimoorthi[7]

[1]Department of Biomedical Science, College of Science, Komar University of Science and Technology, Sulaymaniyah, Kurdistan Region, Iraq.

[2]Department of Pharmacy, College of Medicine, Komar University of Science and Technology, Sulaymaniyah, Kurdistan Region, Iraq.

[3]Regulatory Chemist, Navinta LLC 1499 lower ferry road, Ewing, NJ, USA – 08618.

[4]Department of Pharmaceutics, Sree Sastha pharmacy college, Bangalore high road, Chembarapakkam, Chennai.

[5]Faculty of Pharmaceutical Sciences, PCTE group of institutes, Near Baddowal Cantt, Ferozepur Rd, Punjab 142021.

[6]Srg Hospital and Medical College Jhalawar, Rajasthan, India -326001

[7]Department of Pharmaceutics, Aadhibhagawan college of Pharmacy, Cheyyar.

Cite this paper as: Noel Vinay Thomas, A Salomy Monica Diyya, Shahin Vahora, J.K. Shyamala, Shreya Arora, Harpreet Kaur, Ram C Dhakar ,V. Kalvimoorthi (2024) Preparation and optimization of telmisartan loaded solid lipid nanoparticles by central composite design. *Frontiers in Health Informatics, 13* (7), 90-100

ABSTRACT

Background: Glioblastoma multiforme, commonly known as "glioblastoma," is a rapidly expanding tumor that originates from astrocytes, cells that aid in maintaining the health of brain cells called neuronal cells. Developing, testing, and refining telmisartan solid lipid nanoparticles was the primary objective of the research.

Methods: The fluid injection method was employed to create telmisartan solid lipid nanoparticles. The surfactant was Tween 80, and the lipid was palmitic acid. The drug:lipid ratio and surfactant concentration, which are the formulation's independent factors, were compared to the percentage of drug release and the efficiency of trapping, which are the dependent variables. There were twelve distinct formulations that were evaluated.

Results: To prove that the medication and excipients were compatible, researchers utilized differential scanning calorimetry and Fourier transform infrared spectroscopy. The various telmisartan solid lipid nanoparticles were only a few nanometers in size, yet they were all excellent in enclosing pharmaceuticals and continued to release them for up to twenty-four hours. Scanning electron microscopy revealed the distinctive spherical form of telmisartan solid lipid nanoparticles.

Conclusion: The results of this study show that solid lipid nanoparticles might be a good way to get telmisartan to the brain to treat glioblastoma multiforme.

Keywords: Telmisartan, solid lipid nanoparticles, factorial design, formulation

INTRODUCTION

One form of rapidly expanding tumor is glioblastoma. The star-shaped glial cells that compose it aid in maintaining the health of neurons in the brain. Most people refer to it as a grade IV astrocytoma [1-3]. Brain cancer patients typically succumb to the disease within the first fifteen months after diagnosis. In the brain, glioblastoma multiforme accounts for around 17% of tumors. To treat GBM, surgery is usually the first line of defense. The following steps involve radiation

and chemotherapy [2-4].

Telmisartan (TMS) is the medicine of choice for treating GBM. High-grade invasive glioma and melanoma were determined to respond best to TMS as an anticancer treatment. It is possible for an alkylating substance known as TMS to enter the brain through the bloodstream. The restructured imidazotetrazinone family is its ancestor. Because only 20% of the systemic dosage reaches the brain due to TMS's short half-life of 1.8 hours, large systemic doses are required [3-5].

Greater systemic dosages are required to achieve therapeutic concentrations in the brain. Fatigue, headaches, nausea, vomiting, suppression of bone marrow, and oral ulcers are among the possible adverse effects. Modern drug delivery techniques have been developed to increase the brain's absorption of medications [4-6]. These include nanoparticles, micellar systems, microemulsions, solid lipid nanoparticles, liposomes, niosomes, and many more. They have found a lot of success with medicine delivery to the brain through nanoparticles. Additionally, the increased availability and improved brain penetration caused by the nanometric size of these particle carriers is worth noting. It improves their stability, surface area, and capacity to bind medicines that are water- or fat-loving [5-7].

The following properties of solid lipid nanoparticles (SLNs) have recently attracted a lot of interest: rapid absorption, biocompatibility, biodegradability, reduced dose-dependent toxicity, gradual drug release, long stability, and potential for brain targeting [6-8]. Aqueous detergent solutions or water are the building blocks of sub-micron colloidal carriers (SLN), which are composed of physiological lipids. Their size ranges from fifty nanometers to one thousand nanometers. The Central Composite Design is an advanced layout that combines elements from factorial, fractional, and star layouts. Either a +2k factorial design or a fractional factorial design makes it up [9-13].

Therefore, this study investigated the possibility of administering telmisartan using solid lipid nanoparticles. Using central composite design also allows you to optimize crucial process aspects.

MATERIALS AND METHODS

Materials

A free sample of telmisartan was sent to us by Abbott Pvt. Ltd. in India. We purchased palmitic acid from a Mumbai-based firm known as SD Fine-Chem Ltd. We purchased the soy lecithin from Sigma Aldrich, a Mumbai-based company. All of the chemicals and solvents that were left over were of the laboratory grade.

Methods

Formulation with experimental design

To test the effects of various parameters on the drug release and trapping efficiency, we synthesized batches of solid lipid nanoparticles (SLNs) using the Central Composite Design (CCD). Twelve different formulations were created using a Central Composite Design (CCD) that included 23 factorial experiments. Three distinct levels of randomization were used to evaluate two of the components. Because of their significance to the process, the drug-to-lipid ratio (X2) and surfactant concentration (X1) were selected as independent variables. Because of their significance to SLN quality, we selected entrapment efficiency (R1) and in-vitro drug release (R2) as dependent variables. The limits of concentration are represented by the coded numbers -1.0 for the lower limit and +1.0 for the upper limit. Each design element now features star points that represent new low (-2) and high (+2) numbers. So that it can formulate an effective strategy, the software is programmed with the lowest and maximum values of the processing variables [8-10]. It is possible to view the formulation table and design overview in Table 1.

Table 1: Central Composite Design formulation table

Sr. No.	Batches	Excipients				
		Organic phase		Aqueous phase		
		Drug:Lipid	Ethanol (ml)	Tween-80 (%w/v)	Soya lecithin (g)	Water (ml)
1	B1	1:0	5.0	1.0	1.0	40
2	B2	1:2	5.0	1.5	1.5	40
3	B3	1:3	5.0	2.0	2.0	40
4	B4	1:4	5.0	2.5	2.5	40
5	B5	1:2.0	5.0	1.0	1.0	40
6	B6	1:2.5	5.0	1.5	1.5	40
7	B7	1:1.5	5.0	2.0	2.0	40
8	B8	1:3.0	5.0	2.5	2.5	40
9	B9	1:2.5	5.0	1.0	1.0	40
10	B10	1:3.5	5.0	1.0	2.5	40
11	B11	1:3.2	5.0	3.0	2.0	40
12	B12	1:3.5	5.0	2.0	2.5	40

Preparation of TMS SLNs

Solvent input and ultrasonication were used to make solid lipid nanoparticles. In this method, TMS and palmitic acid (a fatty) were dissolved in ethanol, which made up the organic phase. There are equal amounts of tween 80 (a detergent) and soy lecithin (an emulsifier) in the water phase. With an injection needle, the organic phase was quickly added to the moving water phase, which was then stirred at 1500 rpm for 120 minutes. A probe sonicator was used to sonicate the SLNs suspension for 20 minutes at 50W. The nanosuspension that was made was cooled to 6 °C in order to make TMS SLNs. Separating extra SLNs was done using centrifugation. The SLNs that were bought were kept at low temperatures. Different drug-to-lipid ratios and surfactant amounts were used to make twelve different TMS SLN formulations [14-16].

Evaluation Study

Drug excipient compatibility

FTIR Analysis

To determine the presence of functional groups and the nature of the interactions between the drug and excipients, Fourier transform infrared spectroscopy was employed. Created using potassium bromide discs, FTIR spectra of both the individual medicines and combinations of them were obtained. Ten tons of pressure was applied to a mixture containing potassium bromide or multiple milligrams of telmisartan for five minutes to create the disk. Afterwards, the disk was placed in the FTIR machine's frame, and a spectrum spanning from 4000 cm^{-3} to 500 cm^{-3} was captured [17-21].

DSC Analysis

The process of differential scanning calorimetry (DSC) reveals the melting points of various substances. It is common practice to arrange a DSC experiment's temperature plan such that the sample holder's temperature increases linearly with time. To examine the medication in its pure form as well as in its various mixtures, we utilized a Perkin Elmer Pyris 4 Series DSC apparatus. Metal pans with a volume of 40µl were employed for the samples, while an identical but empty

pan served as a reference. Scan rates of 5°C/min with nitrogen purge rates of 20 ml/min were applied to all samples from 20°C to 320°C [22-26].

Drug Entrapment Efficiency

The TMS-SLNs were centrifuged in a REMI C-854/8 at 3000 rpm for 30 minutes. We employed the subsequent equation to determine the fraction of TMS encapsulated in TMS-SLNs [27-32]:

$$E.E.(\%) = \frac{Total\ amount\ of\ the\ drug - Amount\ of\ the\ free\ drug}{Total\ amount\ of\ the\ drug} \times 100$$

Zeta Potential, PDI, and Particle Size

The average particle diameter and polydispersity index (PDI) were measured at 25°C using the Malvern Zetasizer Nano ZS-V2.0. The samples were diluted by passing them through Milli-Q water that had been filtered using 0.22µm polyvinylidene difluoride filters. The size was determined using DTS-5.10 transparent, single-use measuring cuvettes, with a standard measurement point set at 4.65 mm. The zeta potential is a crucial metric for determining and evaluating the optimal stability conditions of dispersed or colloidal systems. In accordance with the aforementioned equipment, the samples were diluted and probe sonicated prior to the measurements to ensure that there would be no interference during the tests. To conduct the tests at 25 °C, a transparent, disposable zeta cell was filled with water to disperse the particles [33-39].

Surface Morphology study

Scanning electron imaging was employed to examine the nanoparticles' form at an accelerating voltage of 10 kV. The material was attached to a SEM stub using double-sided tape. The coverslips were then coated with conductive carbon paint, and the sample was allowed to dry naturally. The samples were vacuum-coated with a thin layer of gold using a sputter coater in order to reduce the electrostatic charge. Various degrees of magnification were used to capture the images [40-47].

***In-vitro* drug release**

We used a USP-II device to study the drug and TMS SLNs' release in a controlled laboratory environment with phosphate-buffered saline (pH 6.8) as the dissolve medium. At 37°C ± 0.5°C, the medium was mixed while being agitated at 50 rpm. To dissolve the TMS SLN, 100 mg was added to the solution. Substituting five milliliters of fresh medium for the old medium was done at predetermined intervals [48-55]. The absorbance at 325 nm was used to determine the amount of TMS that was generated. The medication release percentage (Y-axis) and the amount of time (X-axis) in hours were plotted to create a graph. This was executed for every version [55-60].

RESULTS AND DISCUSSION

Drug-Excipient compatibility

FTIR studies

The composition and TMS FTIR spectra are shown in Figure 1. Three stretching vibrations were detected: 3180.16 cm-1 for N-H, 3124.99 cm-1 for C-H, and 1744.32 cm-1 for C=O. The drug's functional peaks did not shift noticeably in the TMS SLNs form. Consequently, it was determined that the medication and the excipients did not interfere with one another.

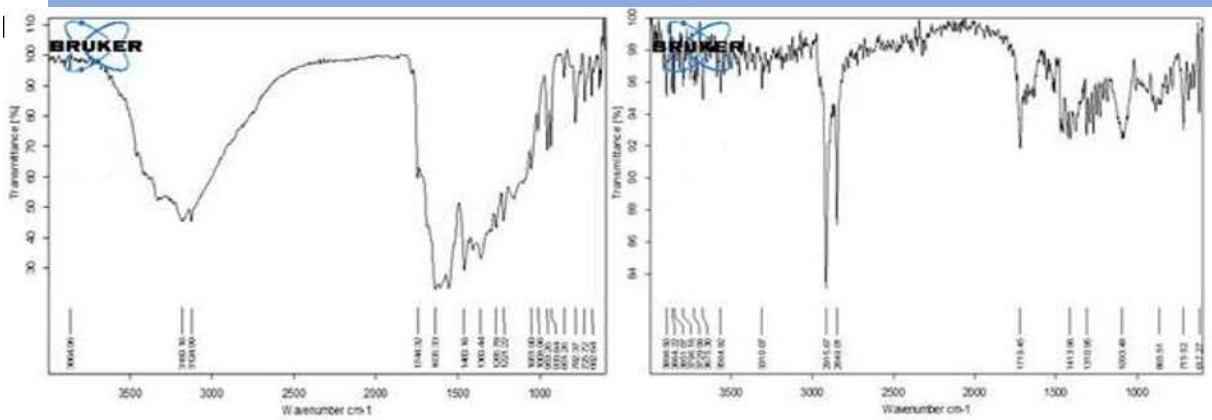

Figure 1: TMS formulation and FTIR spectrum

DSC Analysis

Type of pure DSC drug thermogram and mixture TMS are shown in Figure 2. A DSC peak at 210 °C indicates the melting point of an isolated medicinal compound. An excipient peak at 79.36 °C was observed in the formulation's DSC thermogram, whereas no peaks near the drug's melting point were detected. This meant that the TMS was not crystallized but rather completely encased in the SLNs. On the contrary, it exhibited an amorphous state. In addition, the medicine was unaffected by any of the other components of the concoction.

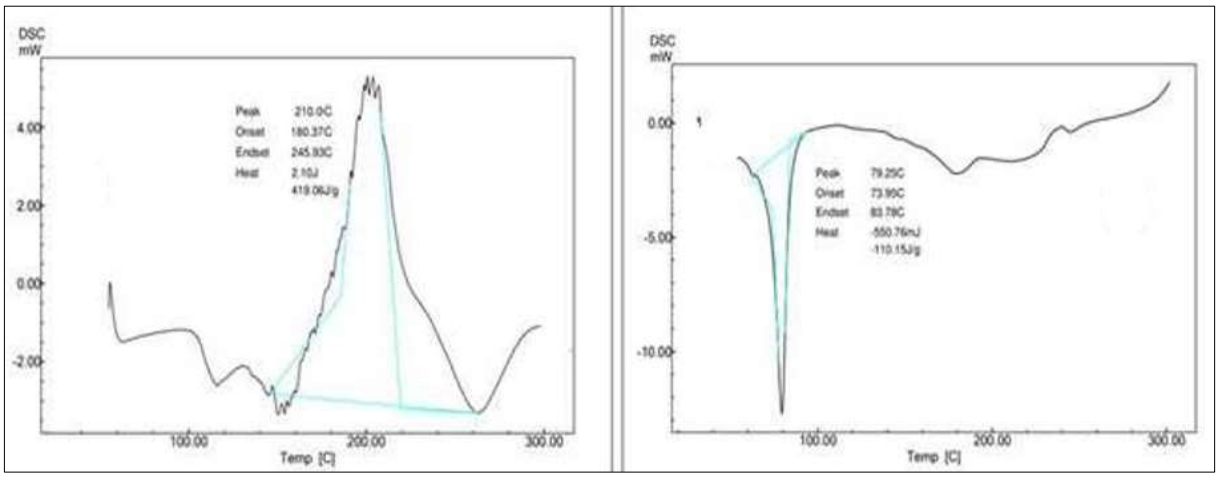

Figure 2: TMS and its formulation DSC thermograms

% EE Efficiency

We made solid lipid nanoparticles (SLNs) and tested their entrapment efficiency, particle size, polydispersity index (PDI), and zeta potential to see how the surfactant concentration and drug-to-lipid ratio affected the SLNs. The entrapment rate of all formulations ranged from 75.614% to 89.126%. The entrapment efficiency went up as the lipid percentage went up. The drug's ability to get stuck in solid lipid nanoparticles (SLNs) got better as the surfactant content went up, but then it got worse again. Increasing the concentration of lipids greatly improved the effectiveness of entrapment by giving the drug more room to stay and lowering its leakage into the external phase. When there are high levels of surfactant, the molecules of the surfactant may not work as well because they get stuck inside the solid lipid nanoparticles.

Table 2: Results of the evaluation of TMS SLNs

Sr. No.	Formulation code	Entrapment efficiency (%)	Particle size (nm)	PDI	Zeta potential (mV)
1	B1	84.254±0.25	379.8	1.124	-71
2	B2	85.76 ±0.36	312.2	1.103	-65
3	B3	82.32±0.46	508.2	1.124	-53
4	B4	86.51±0.31	382.1	1.321	-66
5	B5	75.614±0.71	916.4	1.378	-43
6	B6	89.126±0.55	178.2	1.147	-20
7	B7	81.578±0.34	221.3	1.641	-18
8	B8	85.851±0.86	385.1	1.534	-65
9	B9	86.563±0.37	386.4	1.023	-68
10	B10	86.148±0.92	236.8	1.164	-26
11	B11	85.249±0.86	395.6	1.265	-45
12	B12	85.213±0.89	387.3	1.678	-70

Particle Size, PDI and Zeta Potential

Particle sizes of TMS SLN varied between 178.1 nm and 916.4 nm. The PDI uses the sample size to scale the variability of the data, which ranges from 1.023 to 1.678. Polydispersity occurs when the sizes of a sample are not uniform but instead cluster or agglomerate. A method for determining the surface charge of solid lipid nanoparticles in solution is zeta potential research. The range of zeta potentials seen in TMS SLNs is 18–71.

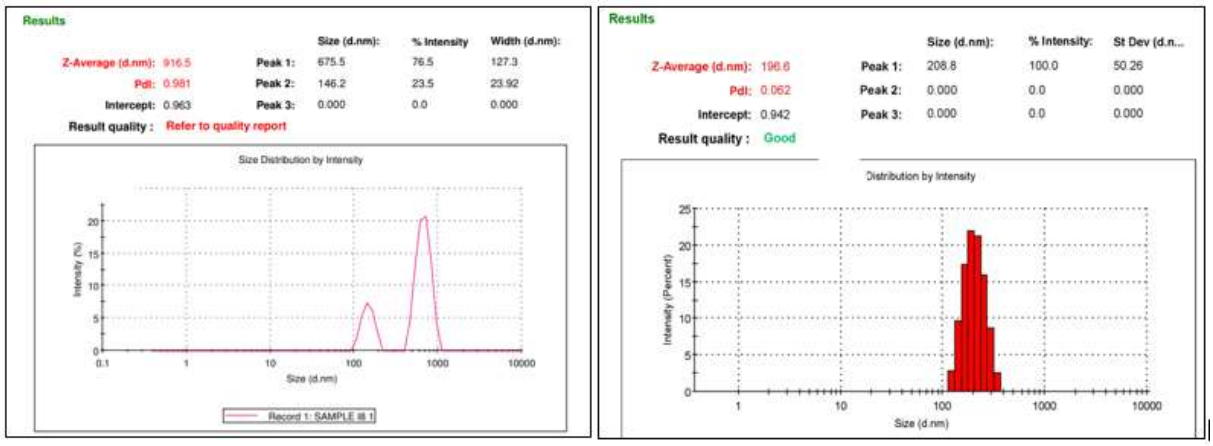

Figure 3: Optimized formulation particle size, PDI, Zeta potential

Surface morphology by SEM

Figure 4 illustrates the results of the morphological observation of TMS SLNs. The results indicated that the solid lipid nanoparticles (SLNs) exhibited a nearly spherical and smooth shape, with an average particle size of 301.3 nm.

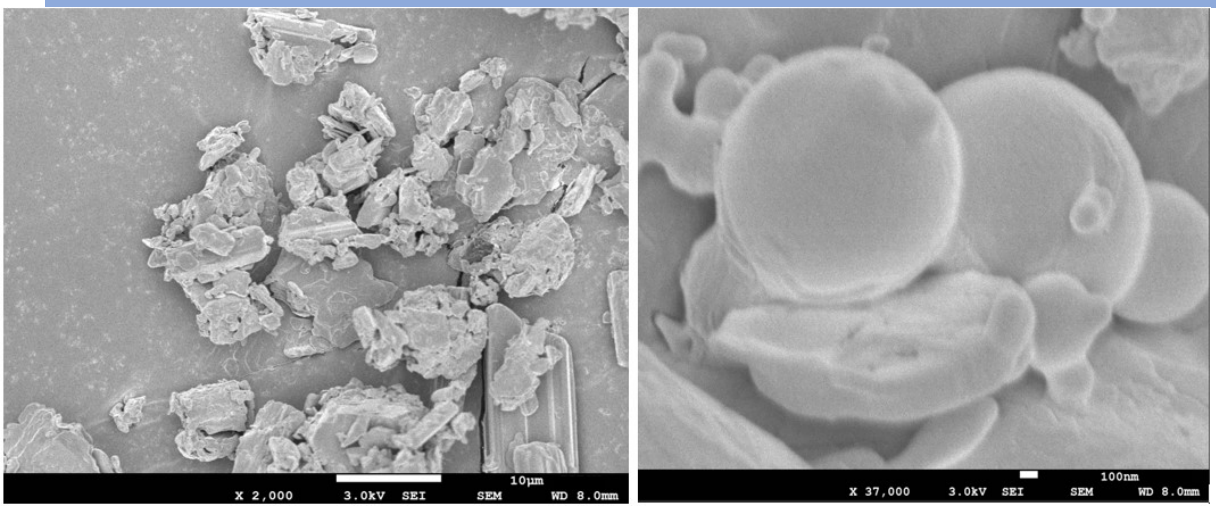

Figure 4: SEM tests of TMS combination and improved formulation

***In-vitro* drug release study**

The drug release properties of all TMS-SLNs were constant in vitro throughout the course of 24 hours. In a 24-hour period, 97.267% of the drug was released by Formulation B6, which contains 1.5% w/v surfactant and a drug-to-lipid ratio of 1:2.50. After the first day, the release from SLNs decreased, but after the second day, it increased again. One possible explanation for the drug's early release could be because TMS eluted off the surface of the SLNs. The gradual diffusion of TMS from the nanoparticles' center may have produced the subsequent continual release. Raising the fat content significantly reduces the overall percentage of medication release. Nanoparticles enlarge with increasing lipid concentrations. Decreased drug release is a result of a smaller surface area that can interact with the releasing medium.

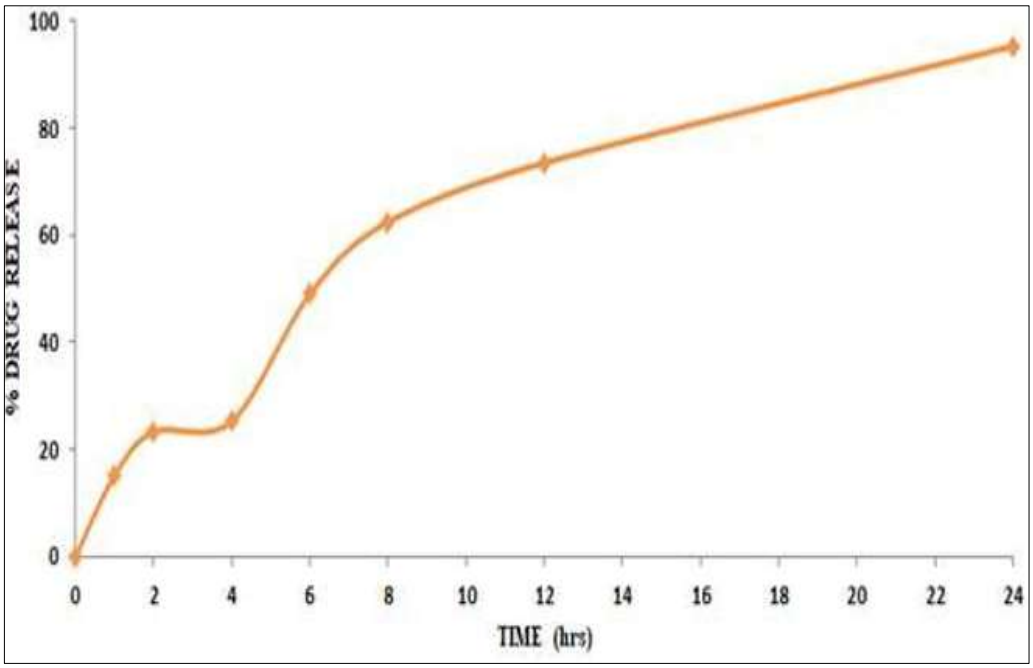

Figure 5: Drug release plot of optimized formulation *in-vitro*

CONCLUSION

The use of a central composite statistical design allowed us to fabricate TMS-loaded SLNs with success. Thanks to this, we were able to determine the optimal surfactant-to-drug-to-lipid ratio for the formulation, allowing for the drug's continuous release throughout the day. The process of TMS release was described using non-Fickian diffusion and first-order dynamics. As a result of using the fictional product, treatment may be less hazardous. Improving their efficacy as a means of administering medication to the brain for the treatment of glioblastoma multiforme requires further research.

Funding
None

Conflict of Interest
None

REFERENCES

1. Son HY, Chae BR, Choi JY, Shin DJ, Goo YT, Lee ES, Kang TH, Kim CH, Yoon HY, Choi YW. Optimization of self-microemulsifying drug delivery system for phospholipid complex of telmisartan using D-optimal mixture design. PLoS One. 2018 Dec 5;13(12):e0208339.
2. Hassan TH, Salman SS, Elkhoudary MM, Gad S. Refinement of Simvastatin and Nifedipine combined delivery through multivariate conceptualization and optimization of the nanostructured lipid carriers. Journal of Drug Delivery Science and Technology. 2021 Aug 1;64:102570.
3. Thapa C, Ahad A, Aqil M, Imam SS, Sultana Y. Formulation and optimization of nanostructured lipid carriers to enhance oral bioavailability of telmisartan using Box–Behnken design. Journal of Drug Delivery Science and Technology. 2018 Apr 1;44:431-9.
4. Nasr M, Kira AY, Saber S, Essa EA, El-Gizawy SA. Telmisartan-Loaded lactosylated chitosan nanoparticles as a liver specific delivery system: synthesis, optimization and targeting efficiency. AAPS PharmSciTech. 2023 Jun 23;24(6):144.
5. Soma D, Attari Z, Reddy MS, Damodaram A, Koteshwara KB. Solid lipid nanoparticles of irbesartan: preparation, characterization, optimization and pharmacokinetic studies. Brazilian Journal of Pharmaceutical Sciences. 2017 Apr 20;53:e15012.
6. Singh VK, Keservani RK. Application of nanoparticles as a drug delivery system. InNovel Approaches for Drug Delivery 2017 (pp. 364-389). IGI Global.
7. Asif AH, Desu PK, Alavala RR, Rao GS, Sreeharsha N, Meravanige G. Development, statistical optimization and characterization of fluvastatin loaded solid lipid nanoparticles: a 32 factorial design approach. Pharmaceutics. 2022 Mar 8;14(3):584.
8. Rout S, Satapathy BS, Sahoo RN, Pattnaik S. Telmisartan loaded lipid nanocarrier as a potential repurposing approach to treat glioma: characterization, apoptosis evaluation in U87MG cells, pharmacokinetic and molecular simulation study. Nanotechnology. 2024 Aug 1;35(42):425101.
9. Öztürk N, Aslı KA, Vural I. Formulation and in vitro evaluation of telmisartan nanoparticles prepared by emulsion-solvent evaporation technique. Turkish Journal of Pharmaceutical Sciences. 2020 Oct;17(5):492.
10. Rajora AK, Ahire ED, Rajora M, Singh S, Bhattacharya J, Zhang H. Emergence and impact of theranostic-nanoformulation of triple therapeutics for combination cancer therapy. Smart Medicine. 2024 Feb;3(1):e20230035.
11. Sharma R, Sardana S, Madan J. Telmisartan loaded Solid Lipid Nanoparticles augmented cytotxicity in cervical cancer cells: Optimization and in vitro characterization. Journal of Drug Delivery and Therapeutics. 2019 Nov 19;9(2):612-24.
12. Ahire E, Thakkar S, Borade Y, Misra M. Nanocrystal based orally disintegrating tablets as a tool to improve

dissolution rate of Vortioxetine. Bulletin of Faculty of Pharmacy, Cairo University. 2020 Dec 1;58(1&2):11-20.
13. Teaima MH, Yasser M, El-Nabarawi MA, Helal DA. Proniosomal telmisartan tablets: formulation, in vitro evaluation and in vivo comparative pharmacokinetic study in rabbits. Drug design, development and therapy. 2020 Mar 31:1319-31.
14. Ahirrao SP, Bhambere DS, Ahire ED, Dashputre NL, Kakad SP, Laddha UD. Formulation and evaluation of Olmesartan Medoxomil nanosuspension. Materials Today: Proceedings. 2023 Jul 1.
15. Ahad A, Raish M, Al-Jenoobi FI, Al-Mohizea AM. Sorbitane monostearate and cholesterol based niosomes for oral delivery of telmisartan. Current drug delivery. 2018 Feb 1;15(2):260-6.
16. Keservani RK, Sharma AK. Nanoemulsions: Formulation insights, applications, and recent advances. Nanodispersions for Drug Delivery. 2018 Sep 24:71-96.
17. Mahajan A, Kaur S. Design, characterization and pharmacokinetic studies of solid lipid nanoparticles of antihypertensive drug Telmisartan. Int J Pharm Sci Res. 2017;8(8):3402-12.
18. Mhetre RL, Hol VB, Dhole SN. Design of Telmisartan Loaded Nanoparticles by Three Square Factorial Design Approach. International Journal of Pharmaceutical and Phytopharmacological Research (eIJPPR). 2018 Aug;8(4):53-62.
19. Khulbe P, Singh DM, Aman A, Ahire ED, Keservani RK. The emergence of nanocarriers in the management of diseases and disorders. Community Acquired Infection. 2023 Apr 19;10.
20. Unnisa A, Chettupalli AK, Al Hagbani T, Khalid M, Jandrajupalli SB, Chandolu S, Hussain T. Development of dapagliflozin solid lipid nanoparticles as a novel carrier for oral delivery: statistical design, optimization, in-vitro and in-vivo characterization, and evaluation. Pharmaceuticals. 2022 May 2;15(5):568.
21. Keservani R, Sharma AK. Self-assembly of sucrose and trehalose alkyl ethers into nanoparticles and nanorods under aqueous conditions. InNanoconjugate Nanocarriers for Drug Delivery 2018 Sep 3 (pp. 515-532). Apple Academic Press.
22. Cho HJ, Lee DW, Marasini N, Poudel BK, Kim JH, Ramasamy T, Yoo BK, Choi HG, Yong CS, Kim JO. Optimization of self-microemulsifying drug delivery system for telmisartan using Box–Behnken design and desirability function. Journal of pharmacy and pharmacology. 2013 Oct;65(10):1440-50.
23. Ahire E, Thakkar S, Darshanwad M, Misra M. Parenteral nanosuspensions: a brief review from solubility enhancement to more novel and specific applications. Acta pharmaceutica sinica B. 2018 Sep 1;8(5):733-55.
24. Teaima M, Abdelmonem R, Adel YA, El-Nabarawi MA, El-Nawawy TM. Transdermal delivery of telmisartan: formulation, in vitro, ex vivo, iontophoretic permeation enhancement and comparative pharmacokinetic study in rats. Drug design, development and therapy. 2021 Nov 10:4603-14.
25. Keservani RK, Sharma AK, Kesharwani RK. Nanoparticulate nanocarriers in drug delivery. InNanobiomaterials 2018 Jan 3 (pp. 3-22). Apple Academic Press.
26. Tiwari G, Gupta M, Devhare LD, Tiwari R. Therapeutic and phytochemical properties of thymoquinone derived from Nigella sativa. Curr Drug Res Rev., 16, 145–156 (2024).
27. Tiwari R, Khatri C, Tyagi LK, Tiwari G. Expanded therapeutic applications of Holarrhena antidysenterica: A review. Comb Chem High Throughput Screen., 27, 1257–1275 (2024).
28. Tiwari G, Tiwari R, Kaur A. Pharmaceutical considerations of translabial formulations for treatment of Parkinson's disease: A concept of drug delivery for unconscious patients. Curr Drug Deliv., 20, 1163–1175 (2023).
29. Tiwari R, Tiwari G, Parashar P. Theranostics applications of functionalized magnetic nanoparticles. In Multifunctional and targeted theranostic nanomedicines: Formulation, design and applications. Singapore: Springer Nature Singapore., 361–382 (2023).
30. Tiwari R, Mishra J, Devhare LD, Tiwari G. An updated review on recent developments and applications of fish

collagen. Pharma Times, 55, 28–30 (2023).
31. Tiwari R, Tiwari G, Mishra S, Ramachandran V. Preventive and therapeutic aspects of migraine for patient care: An insight. Curr Mol Pharmacol., 16, 147–160 (2023).
32. Tiwari R, Pathak K. Local drug delivery strategies towards wound healing. Pharmaceutics, 15, 634 (2023).
33. Tiwari R, Tiwari G, Sharma S, Ramachandran V. Exploration of herbal extract-loaded phyto-phospholipid complexes (phytosomes) against polycystic ovarian syndrome: Formulation considerations. Pharm Nanotechnol., 11, 44–55 (2023).
34. Tiwari G, Chauhan A, Sharma P, Tiwari R. Nutritional values and therapeutic uses of Capra hircus milk. Int J Pharm Investig., 12, (2022).
35. Dhas N, García MC, Kudarha R, Pandey A, Nikam AN, Gopalan D, et al. Advancements in cell membrane camouflaged nanoparticles: A bioinspired platform for cancer therapy. J Control Release, 346, 71–97 (2022).
36. Tiwari R, Tiwari G, Lahiri A, Ramachandran V, Rai A. Melittin: A natural peptide with expanded therapeutic applications. Nat Prod J., 12, 13–29 (2022).
37. Tiwari G, Singh G, Shekhar R, Tiwari R. Development and qualitative evaluation of periodontal gel containing an antibacterial agent for periodontal disease. Res J Pharm Technol., 15, 5225–5231 (2022).
38. Tiwari R, Rathour K, Tyagi LK, Tiwari G. Eggshell: An essential waste product to improve dietary calcium uptake. Pharmacophore, 13, 32–40 (2022).
39. Tiwari R, Singh I, Gupta M, Singh LP, Tiwari G. Formulation and evaluation of herbal sunscreens: An assessment towards skin protection from ultraviolet radiation. Pharmacophore, 13, 41–49 (2022).
40. Kaur A, Tiwari R, Tiwari G, Ramachandran V. Resveratrol: A vital therapeutic agent with multiple health benefits. Drug Res., 72, 5–17 (2022).
41. Tiwari G, Tiwari R. Assessment of nutraceutical potential of herbs for promoting hair growth: Formulation considerations of herbal hair oil. Open Dermatol J., 15, (2021).
42. Tiwari R, Lahiri A, Tiwari G, Vadivelan R. Design and development of mupirocin nanofibers as medicated textiles for treatment of wound infection in secondary burns. Int J Pharm Sci Nanotechnol., 14, 5672–5682 (2021).
43. Singh S, Tiwari R, Tiwari G. Importance of artificial intelligence in the medical device and healthcare sector. Pharma Times, 53, 21–24 (2021).
44. Tiwari R, Tiwari G, Yadav A, Ramachandran V. Development and evaluation of herbal hair serum: A traditional way to improve hair quality. Open Dermatol J., 15, (2021).
45. Tiwari R, Tiwari G, Ramachandran V, Singh A. Non-conventional therapy of lethal pneumonia symptoms and viral activity of SARS-CoV-2 during COVID-19 infection using bee venom compound, melittin: A hypothesis. Pharma Times, 53, 14–18 (2021).
46. Tiwari R, Wal P, Singh P, Tiwari G, Rai A. A review on mechanistic and pharmacological findings of diabetic peripheral neuropathy including pharmacotherapy. Curr Diabetes Rev., 17, 247–258 (2021).
47. Tiwari R, Tiwari G, Lahiri A, Vadivelan R, Rai AK. Localized delivery of drugs through medical textiles for treatment of burns: A perspective approach. Adv Pharm Bull., 11, 248 (2021).
48. Tiwari R, Tiwari G, Singh R. Allopurinol-loaded transferosomes for the alleviation of symptomatic after-effects of gout: An account of pharmaceutical implications. Curr Drug Ther., 15, 404–419 (2020).
49. Shukla R, Tiwari G, Tiwari R, Rai AK. Formulation and evaluation of the topical ethosomal gel of melatonin to prevent UV radiation. J Cosmet Dermatol., 19, 2093–2104 (2020).
50. Tiwari G, Tiwari R, Singh R, Rai AK. Ultra-deformable liposomes as flexible nanovesicular carrier to penetrate versatile drugs transdermally. Nanosc Nanotechnol-Asia, 10, 12–20 (2020).
51. Patel M, Thakkar A, Bhatt P, Shah U, Patel A, Solanki N, et al. Prominent targets for cancer care:

Immunotherapy perspective. Curr Cancer Ther Rev., 19, 298–317 (2023).
52. Patel BA. Permeation enhancement and advanced strategies: A comprehensive review of improved topical drug delivery. Int Res J Mod Eng Technol Sci., 6, 6691–6702 (2024).
53. Patel BA. Niosomes: A promising approach for advanced drug delivery in cancer treatment.
54. Shah U, et al. Atorvastatin's reduction of Alzheimer's disease and possible alteration of cognitive function in midlife as well as its treatment. CNS Neurol Disord Drug Targets, 22, 1462–1471 (2023).
55. Patel N, et al. Investigating the role of natural flavonoids in VEGFR inhibition: Molecular modeling and biological activity in A549 lung cancer cells. J Mol Struct., 1322, 140392 (2025).
56. Vijapur LS, et al. Formulation standardization and quality control of polyherbal formulation for treatment of type 2 diabetes mellitus. Nanotechnol Percept., 20, 775–783 (2024).
57. Patel V, et al. Eco-friendly approaches to chromene derivatives: A comprehensive review of green synthesis strategies. Curr Top Med Chem., (2024).
58. Patil A, et al. Preparation, optimization, and evaluation of ligand-tethered atovaquone-proguanil-loaded nanoparticles for malaria treatment. J Biomater Sci Polym Ed., 1–32 (2024).
59. Patel BA, Sachdeva PD. Evaluations of anti-asthmatic activity of roots of Moringa oleifera Lam. in various experimental animal models. Inventi Impact Planta Activa, (2011).
60. Patel D, et al. Review on therapeutic diversity of oxazole scaffold: An update. ChemSelect, 9, e202403179 (2024).